MOLECULAR AND CELLULAR BIOLOGY, Oct. 1994, p. 6773–6788
0270-7306/94/$04.00+0

Vol. 14, No. 10

BZP, a Novel Serum-Responsive Zinc Finger Protein That Inhibits Gene Transcription

ALAN J. FRANKLIN, THOMAS L. JETTON, KATHY D. SHELTON, AND MARK A. MAGNUSON*

Department of Molecular Physiology and Biophysics, Vanderbilt University Medical School, Nashville, Tennessee 37232

Received 20 April 1994/Returned for modification 31 May 1994/Accepted 7 July 1994

We report the fortuitous isolation of cDNA clones encoding a novel zinc finger DNA-binding protein termed BZP. The protein encoded is 114 kDa and contains eight zinc finger motifs, seven of which are present in two clusters at opposite ends of the molecule. Both finger clusters bound to the 9-bp sequence AAAGGTGCA with apparent K_ds of ~2.5 nM. Two of the finger motifs within the amino- and carboxy-terminal finger clusters share 63% amino acid identity. BZP inhibited transcription of the herpes simplex virus thymidine kinase promoter when copies of the 9-bp target motif were linked in *cis*, suggesting that it functions as a transcriptional repressor. BZP mRNA and immunoreactivity were detected in several established cell lines but were most abundant in hamster insulinoma (HIT) cells, the parental source of the cDNAs. In mouse tissues, BZP mRNA and immunoreactivity were identified in cells of the endocrine pancreas, anterior pituitary, and central nervous system. Interestingly, in HIT cells proliferating in culture, BZP immunoreactivity was predominately nuclear in location, whereas it was usually located in the cytoplasm in most neural and neuroendocrine tissues. Serum deprivation of HIT cells caused BZP immunoreactivity to become predominately cytoplasmic in location and attenuated its inhibitory effect on transcription, thereby suggesting that the both the subcellular location and the function of this protein are modulated by factors in serum.

Zinc finger-containing proteins contribute to transcriptional regulation of a wide variety of gene products (4, 11, 19, 65). This DNA binding motif was first identified in TFIIIA, a transcription factor that binds the *Xenopus* 5S RNA gene (5, 9); several subclasses, the C_2C_2 (11, 18), CCHC (4, 65), and C_2H_2 (50) zinc finger motifs, have subsequently been identified. Many proteins containing C_2H_2 zinc finger motifs have now been cloned from multiple species. Representative examples include Xfin (48), Krüppel (47), Hunchback (60), GATA-1 (61), Krox (6), TDF (38), and the GLI family of zinc finger proteins (27). There is convincing evidence that many C_2H_2 finger proteins are essential for normal growth and development. For instance, mutations in Krüppel lead to deformities of the anterior abdominal and thoracic regions in *Drosophila melanogaster* (42), and targeted mutations of GATA-1 in chimeric mice block erythroid cell differentiation (41). Moreover, C_2H_2 zinc finger proteins have also been implicated in the pathogenesis of human disease (15, 63).

Modulation of the amount and/or location of transcription factors is, in general, an important way of regulating their activity during cellular growth and development. In some cases, the quantity of protein within the cell is altered by either transcriptional or posttranscriptional mechanisms. Examples include the induction by serum of the PRDII-BF1 gene (12), activation during the G_0/G_1 transition of the *Krox-20* gene (7), and the coregulation with c-*fos* following growth factor and mitogenic stimuli of the *egr-1/Krox-24* gene (59). In other cases, the subcellular localization of preexisting protein is modulated. The glucocorticoid receptor, for instance, is a well-characterized example of a zinc finger protein that changes its subcellular location from the cytoplasm to nucleus in response to hormone binding. Protein phosphorylation is known to play a role in altering the subcellular location of certain DNA-binding proteins (for a review, see reference 21). For instance, both the nuclear transport and function of SWI5, a C_2H_2 zinc finger protein from *Saccharomyces cerevisiae* (58), are under cell cycle control (10, 34) and change in response to phosphorylation at three $p34^{cdc2}$ consensus sites within or near its nuclear localization sequence (34).

Phosphorylation of the NF-κB/Iκ-B, dorsal/cactus, and Rel families of proteins through various signal transduction pathways plays a central role in their nuclear entry and function (17). NF-κB is sequestered in the cytoplasm by an interaction with Iκ-B (3, 16). Phosphorylation causes the dissociation of the NF-κB/Iκ-B complex, thereby freeing NF-κB to translocate to the nucleus and affect gene transcription. The *Drosophila* homologs of NF-κB and Iκ-B, dorsal and cactus, possess a similar molecular regulation (1). A gradient of dorsal nuclear localization is established early in development in which the dorsal protein is found predominantly within the nuclei of ventrally located cells but within the cytoplasm of dorsally located cells (56, 57). Cactus associates with dorsal, thereby sequestering the complex in the cytoplasm, analogous to the interactions of NF-κB with Iκ-B (14, 26). Phosphorylation of dorsal by Toll receptor-activated protein kinase A leads to a nuclear localization of the protein, thereby permitting it to transactivate target genes (37).

In this report, we describe the fortuitous cloning of a novel 114-kDa C_2H_2 zinc finger protein termed BZP. Clones for BZP were obtained in an attempt to clone an unrelated ~50-kDa protein that is expressed in pancreatic β cells and binds to the upstream promoter elements (UPEs) in the upstream glucokinase promoter. Analysis of the DNA-binding specificity of BZP revealed that by multimerizing the double-stranded DNA probe used for library screening, a 9-bp DNA element to which BZP binds was created. We have determined that while BZP is distinct from the sought-after DNA-binding protein, it is nevertheless found within the nuclei of insulinoma cells growing in culture and the cytoplasm of the mouse

* Corresponding author. Mailing address: 702 Light Hall, Vanderbilt University School of Medicine, Nashville, TN 37232. Phone: (615) 322-7006. Fax: (615) 322-7236.

endocrine pancreas. Further, the subcellular distribution pattern of BZP varies in different mouse tissues and is altered in HIT M2.2.2 cells by serum starvation. Thus, while BZP clones were not those originally sought, various features of this novel protein prompted us to analyze its DNA binding specificity, tissue distribution, and subcellular localization.

MATERIALS AND METHODS

General procedures. All DNA manipulations were accomplished by using standard procedures (33) unless otherwise noted. Oligonucleotide primers were synthesized by either Midland Reagent Co. (Midland, Tex.) or the Vanderbilt DNA Core Laboratory. RNA was isolated by the AGCP method (8) and fractionated to poly(A)$^+$ RNA by oligo(dT) chromatography. Nucleic acid sequence was obtained by dideoxynucleotide chain termination reactions using Sequenase II (U.S. Biochemicals). Both strands of all four cDNA clones were sequenced.

cDNA expression libraries and screening. A cDNA library in λZAPII (Stratagene) was made as instructed by the supplier, using poly(A)$^+$ RNA isolated from HIT M2.2.2 cells, and amplified once prior to use. Another HIT M2.2.2 cell cDNA library in λgt11 was the gift of L. Moss (Tufts University, New England Medical Center). A total of 900,000 plaques from these libraries were screened by the method of Singh et al. (54), using a concatemerized oligonucleotide pair that contained upstream glucokinase promoter sequences from −139 to −124. The oligonucleotide pair was synthesized with nonsymmetric 5′ overhangs that allowed the annealed DNA to be unidirectionally ligated. The probe contains UPE-2 (shown in boldface), which is the binding site for a β-cell-specific factor of ~50 kDa (53). The sequence of the probe is as follows:

5′-TGCACCTTTGGC**CATCAG**
GGAAACCG**GTAGTC**AGCT-5′

The oligonucleotide pair was annealed by heating to 100°C and then cooled over 1 h to room temperature. The probe was radiolabeled and multimerized by the procedure of Vinson et al. (62).

RNA blot analysis. Ten micrograms of poly(A)$^+$ RNA was separated on a denaturing agarose gel containing 7% formaldehyde. The RNA was capillary blotted to nitrocellulose and cross-linked, using 1,200 mJ of UV light. The blot was prehybridized for 16 h at 45°C in 50% formamide–5× Denhardt's solution–1× SSPE (1× SSPE is 0.18 M NaCl, 10 mM NaH_2PO_4, and 1 mM EDTA [pH 7.7])–0.5% sodium dodecyl sulfate (SDS)–10 μg of denatured salmon sperm DNA per ml before hybridization for 16 h at 45°C with 200 ng of a cDNA probe labeled by random priming with [α-^{32}P]dATP to a specific activity of 0.5×10^9 to 1.0×10^9 cpm/μg of DNA. Autoradiography was performed after three washes for 10 to 15 min each at 60 to 65°C in 0.2× SSC (1× SSC is 0.15 M NaCl plus 0.015 M sodium citrate)–0.1% SDS.

Protein expression and purification. BZP cDNA 5 was altered by the site-specific mutagenesis method of Kunkel (30) to introduce either an *Xho*I or a *Bam*HI restriction endonuclease site (underlined below) to allow ligation of cDNA subfragments into pET15b, a procaryotic expression vector containing an amino-terminal histidine repeat (Novagen). For expression of full-length BZP, the mutating oligonucleotides were 5′-GTGGCATGCTCGAGGATGA and 5′-TGAAGCC TAGGATCCCTTCTAGAAGGA. For pET-1, the mutating oligonucleotides were 5′-GTGGCATGCTCGAGGATGA and 5′-AATAAACCCCTTTAGGATCCGCTTTCTGTA. For pET-2, the mutating oligonucleotides were 5′-GGAGTCTC CACACTCGAGGACCAGAAG and 5′-TGAAGCCTAGGA TCCCTTCTAGAAGGA. Correct mutagenesis was verified by DNA sequencing and restriction endonuclease digestion before expression in *Escherichia coli* BL21 (DE3). The fusion protein was expressed by growing the bacteria to an A_{600} of 0.6 to 0.8 and inducing expression with 1 mM isopropylthiogalactopyranoside (IPTG) for 2 to 3 h at 30°C. The cells were pelleted at 300 × *g* for 20 min at 4°C and resuspended in protein resuspension buffer containing 20 mM Tris (pH 7.5), 0.5 M sodium chloride, 5 mM imidazole, 10% glycerol, and 1 mM phenylmethylsulfonyl fluoride. The cells were lysed by incubation for 10 min at 22°C with protein resuspension buffer containing 100 mg of chicken egg white lysozyme and 0.1% Triton X-100 followed by sonication for 1 min at 4°C. Following centrifugation at 14,000 × *g* for 20 min at 4°C, the supernatant fraction was filtered through a 0.45-μm-pore-size filter and subjected to nickel affinity chromatography to partially purify the expressed fusion protein. The bacterial supernatant was loaded onto a 2.5-ml nickel column (Novagen) and washed with at least 10 column volumes of protein resuspension buffer. Nonspecific protein-column interactions were reduced further by three 10-ml washes of protein resuspension buffer with 20, 40, and 60 mM imidazole, respectively. Fusion protein was eluted in protein resuspension buffer containing 130 mM imidazole, and its purity was assessed by SDS-polyacrylamide gel electrophoresis (PAGE). A 1:500 dilution of an inhibitor cocktail containing aprotonin (1 mg/ml), antipain (1 mg/ml), leupeptin (1 mg/ml), chymostatin (1 mg/ml), pepstatin A (1 mg/ml), trypsin-chymotrypsin inhibitor (5 mg/ml), and 50 mM benzamidine was added to fractions, which were dialyzed twice for 45 min each time against a 500-fold volume excess of a solution containing 20 mM *N*-2-hydroxyethylpiperazine-N′-2-ethanesulfonic acid (HEPES; pH 7.8), 10 mM potassium chloride, 2 mM dithiothreitol, 100 μM $ZnSO_4$, and 5% glycerol and used in DNA binding studies.

Linker-primer PCR was used to generate cDNA fragments from BZP cDNA 5 that contained *Bam*HI and *Eco*RI restriction endonuclease sites (underlined below) at the 5′ and 3′ ends, respectively, for ligation into pGEX-2T, a procaryotic expression vector that produces a fusion protein with *Schistosoma japonicum* glutathione *S*-transferase (GST). For pGST-1, the primers 5′-CCGGATCCTCAAGACATCGCAGTGT (top) and 5′-CCGAATTCTGATTTAACAGTAAG (bottom) were used. For pGST-2, the primers 5′-CCGGATCCTCCTATCG CTCTTAAA (top) and 5′-CCGAATTCTGAGTCTGTAACA CA (bottom) were used. After expression in *E. coli*, the recombinant peptides were purified by GST-agarose affinity chromatography (55).

Gel mobility shift assays and DNase I footprinting. DNA-protein binding reactions were performed as described previously (53) except that 100,000 cpm of ^{32}P-labeled DNA probe was used with 1 μg of purified recombinant peptide. The reaction products of gel mobility shift assays were fractionated in 4% nondenaturing polyacrylamide gels. To measure the apparent K_d, an excess of BZP binding peptide was used so that DNA-protein binding would not affect overall protein concentration. Hence, each DNA binding reaction mixture contained either 100 ng of pET-1 peptide or 40 ng of pET-2 peptide and 1 μg of bovine serum albumin (BSA) to decrease nonspecific protein binding. Bound counts were measured directly by using a PhosphorImager (Molecular Dynamics) and plotted against total DNA concentration. In cold competition assays, a 25-fold excess of unlabeled competitor DNAs was preincubated with the finger motif peptides for 20 min at 4°C before the radiolabeled DNA probe was added. For DNase I

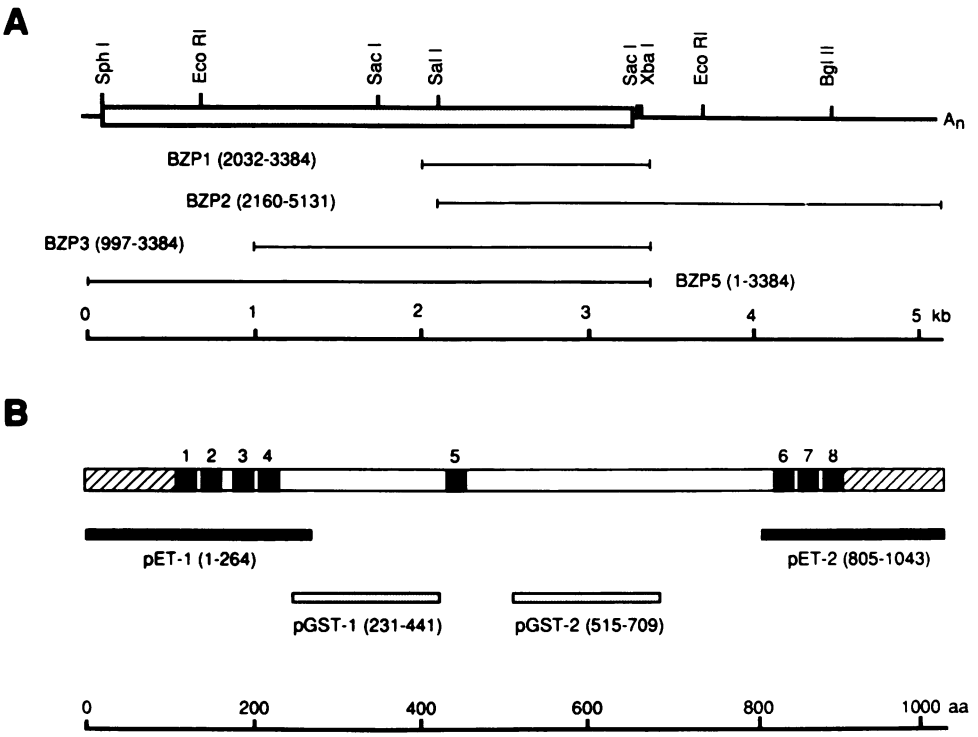

FIG. 1. Restriction map of cDNA clones and structural features of the encoded protein. (A) Restriction endonuclease maps of the four overlapping cDNAs obtained by using a Southwestern expression screening strategy. The boxed area indicates the open reading frame of the protein. The endpoints of each clone relative to the total sequence are indicated in parentheses. (B) Locations of the zinc finger motifs (black boxes) and acidic regions (cross-hatched regions) in BZP. The peptides expressed in *E. coli* for use as immunogens (white) and for DNA binding experiments (black) are shown. The endpoints relative to the entire protein of 1,043 amino acids are indicated.

footprinting, $CaCl_2$ was added to a concentration of 1 mM after the protein binding reactions, and partial DNase I digestion was performed by incubation with 25 ng of DNase I (Worthington) in a total volume of 30 μl for 5 min at 22°C. Digestion was stopped by adding 10 μl of stop solution containing 1 M sodium chloride, 100 mM Tris (pH 7.5), 15 mM EDTA, 2% SDS, and 7 μg of proteinase K for 15 min at 37°C. The DNA fragments were precipitated with ethanol, and the pellet was resuspended in 300 mM sodium acetate, precipitated again with ethanol, washed with 70% ethanol at −20°C, and then resuspended in 5 μl of loading buffer. The resulting samples and Maxam and Gilbert G+A reaction mixtures were boiled for 5 min prior to electrophoresis on a 6% denaturing polyacrylamide gel. After electrophoresis, the gels were dried and autoradiographed, and the footprinted sequence was deduced from the G+A cleavage patterns.

Methylation interference assay. A three-copy multimer of the screening oligonucleotide was cloned into the *Eco*RV site of pBlueScript M13+ (Stratagene) by using Klenow fragment to blunt the ligated oligonucleotides prior to vector ligation. The plasmid was linearized with either *Bam*HI or *Xho*I and filled in with [α-^{32}P]dATP, using the Klenow fragment of DNA polymerase I to label the probe at one or the other end, and then the plasmid was digested with the complementary enzyme to release the labeled 114-bp DNA fragment. This fragment was purified by elution from a 4% nondenaturing polyacrylamide gel and partially methylated by incubation with 1 μl of dimethyl sulfate and 50 mM sodium cacodylate for 90 s at 22°C. Methylation was stopped by the addition of sodium acetate (pH 5.2) and 2-mercaptoethanol to concentrations of 500 and 333 mM, respectively, and the DNA was precipitated twice with ethanol. Binding reaction mixtures contained 4 × 10^6 cpm of one end-labeled probe, 3 μg of poly(dI-dC), 6 μg of denatured salmon sperm DNA, and either 10 μg of pET-1 or 1.5 μg of pET-2 partially purified protein. The remaining steps were performed as described previously (53) except that fractionation of the DNA following piperidine cleavage was performed with a 6% denaturing polyacrylamide gel that was dried before autoradiography.

Transfection assays. Transient transfections of HIT M2.2.2 and NIH 3T3 cells were performed as described by Shelton et al. (53), and cells were harvested 20 to 36 h after glycerol shock. Transfection efficiencies were normalized by measuring activity from either 1 μg of Rous sarcoma virus–β-galactosidase or 2 μg of simian virus 40 (SV40)–β-galactosidase expression vector cotransfected with the test plasmids. An overlapping oligonucleotide pair with the sequence

5′-GATCTGGCC**AAAGGTGCA**G
ACCGG**TTTCCACGT**CCTAG-5′

that contained a single BZP binding site (in boldface) was ligated in molar excess to a *Bam*HI site upstream of a minimal herpes simplex virus thymidine kinase promoter (−32 to +51) driving a luciferase reporter gene (designated TK-luc), and clones containing one, three, and five copies of the binding site were identified. An *Xba*I fragment of BZP cDNA 5 was ligated into the *Xba*I site of pCMV4 (2) to create pCMV-BZP. Cotransfection assays with the pCMV-BZP expression vector and target site reporter were performed using 5 μg of the TK-luc plasmids in addition to 2.5 μg of either pCMV4 or pCMV-BZP in HIT M2.2.2 cells and 10 μg of the TK-luc

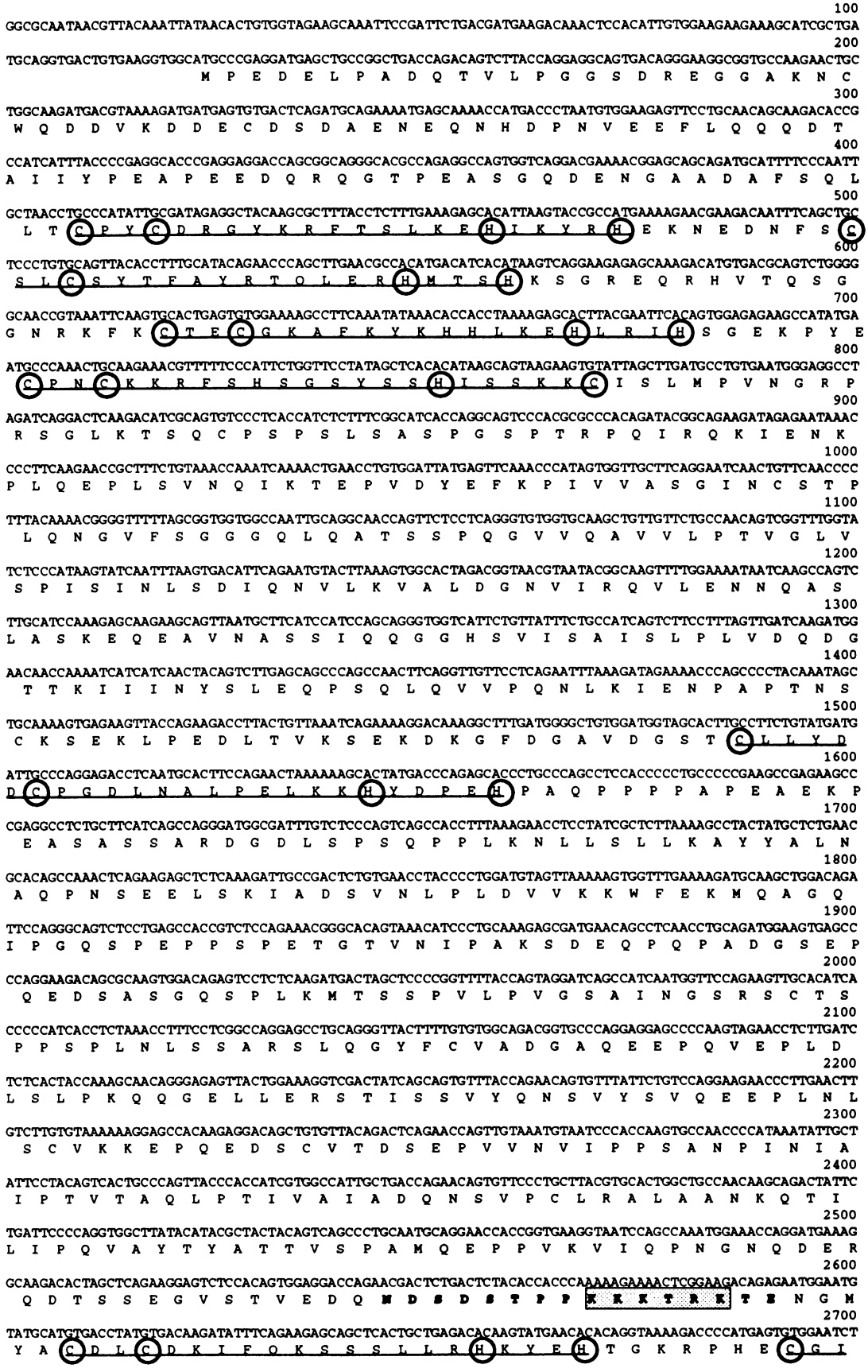

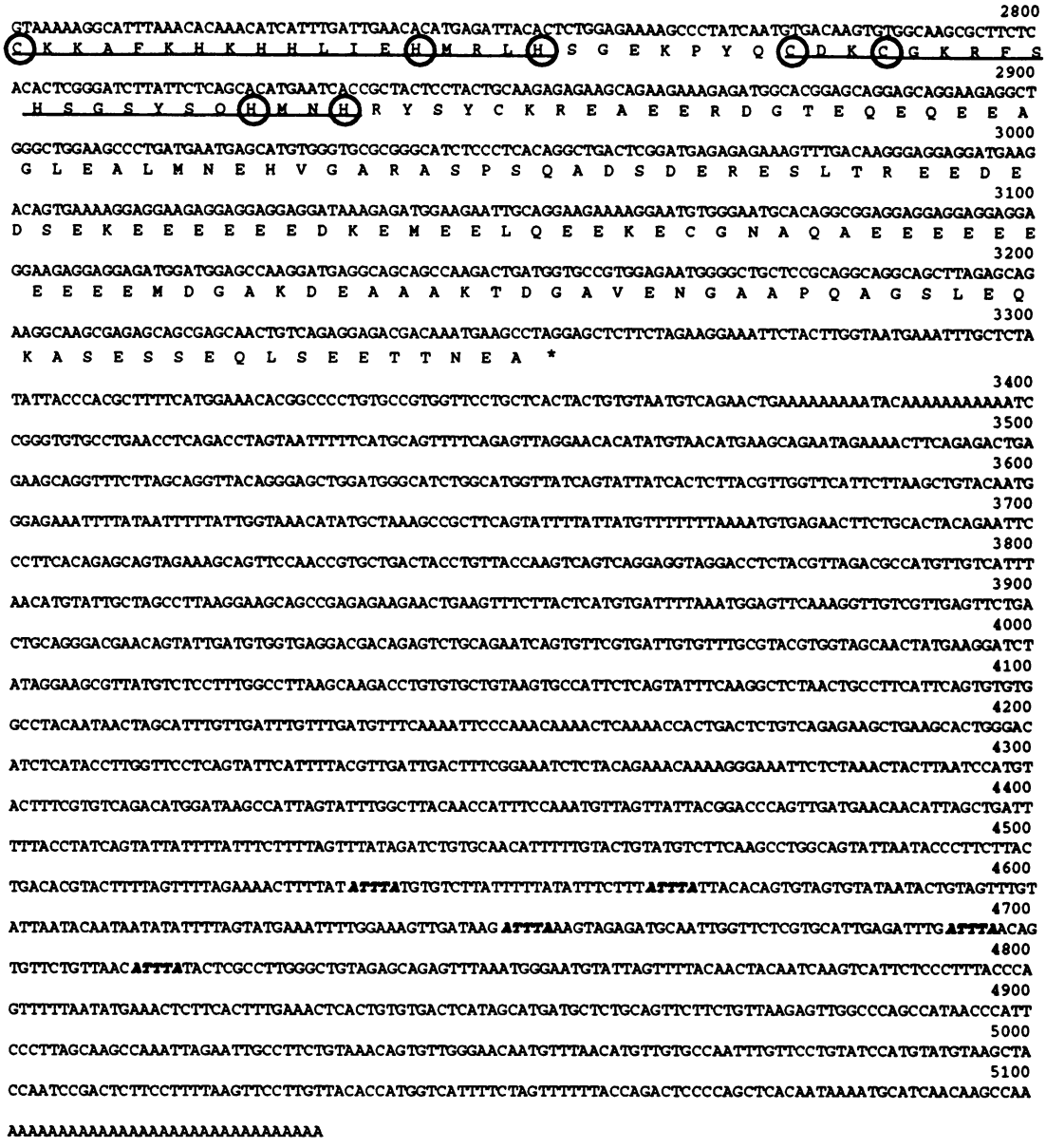

FIG. 2. Nucleic acid and deduced amino acid sequences of BZP. The zinc finger motifs in the protein are underlined, and the cysteine and histidine residues that may be involved in chelating a zinc ion are circled. Five AUUUA repeats in the 3′ untranslated sequence are shown in an italicized boldface font. A putative nuclear translocation signal is boxed. The protein was also found to contain multiple consensus phosphorylation sites for protein kinases A and C, casein kinase II, and $p34^{cdc-2}$ kinase (25).

plasmids in addition to 5 μg of either pCMV4 or pCMV-BZP in NIH 3T3 cells.

Immunoblot analysis. Nuclear and cytoplasmic extracts from HIT cells that were incubated in medium with or without serum for 24 h were prepared and fractionated on an SDS–7.5% polyacrylamide gel. The gel was electroblotted onto an Immobilon-P membrane, briefly hydrated in phosphate-buffered saline (PBS) (pH 7.4), blocked overnight in PBS containing 5% instant dry milk (Carnation) and 0.02% NaN_3 at 4°C, washed again in PBS, and then incubated overnight at 4°C in PBS containing 2% dry milk and 0.02% NaN_3 with either a 1:4,000 dilution of preimmune serum or anti-BZP immunoglobulin G (IgG) at a concentration of 0.1 to 1.0 μg/ml. After three washes for at least 15 min each in PBS, the samples were allowed to incubate in PBS containing 3% BSA and 2 to 3 μg of biotinylated goat anti-rabbit antibody (Jackson ImmunoResearch) per ml for 2 h at 22°C. Unbound antibody was removed by three washes for at least 45 min each with PBS, and then a 1:100 dilution of streptavidin-peroxidase (BioGenex) was added for 1 h at 22°C. Following three washes with PBS for 10 to 15 min each and equilibration in 10 mM sodium citrate (pH 5.0)–10 mM EDTA, dextran sulfate was added to a concentration of 1% of 10 min and removed by three washes buffer alone for 5 min each, and then the blots were developed for 10 to 15 min in the presence of 3,3′,5,5′-tetramethylbenzidine (Boehringer Mannheim) and hydrogen peroxide at concentrations of 20 μg/ml and 0.05%, respectively.

Immunocytochemistry. (i) Tissue fixation. Tissues from 8- to 12-week-old mice or whole neonatal mice were fixed, processed, and sectioned as described previously (24). Endogenous peroxidase activity was blocked prior to immunoperoxidase experiments as previously described (24), and endogenous avidin and biotin were blocked as recommended by the manufacturer (Zymed Laboratories).

(ii) Antisera to BZP. The pGST-1- and pGST-2-generated fusion peptides were used as immunogens in rabbits to produce four different lots of antisera (Bethyl Laboratories). The IgG component of each of these antisera was isolated by recombinant protein G-agarose chromatography (Pierce Immunochemical), and the IgG fractions were further adsorbed against an immobilized *E. coli* lysate (Pierce Immunochemical) to minimize potential cross-reactivity. Of the four animals immunized, antisera from two were discarded because of presensitization against islet cell antigens and were unsuitable for immunolocalization studies. Thus, sera from only two animals, 2433 (anti-peptide 1) and 2397 (anti-peptide 2), were used.

(iii) Cell line immunostaining. All incubations and washes were at 22°C unless otherwise noted. HIT M2.2.2 cells were grown on coverslips in Dulbecco's modified essential medium supplemented with 15% (vol/vol) horse serum, 2.5% (vol/vol) fetal calf serum, and 50 μg each of streptomycin and penicillin per ml. After incubation in medium with or without serum, the cells were fixed in PBS containing 4% paraformaldehyde for 20 min, washed three times in PBS for 5 to 10 min each, and then permeabilized with 0.2% Triton X-100 in PBS for 20 min. Following a wash in PBS, nonspecific binding was blocked by incubation first in PBS containing 3% BSA and then in PBS containing 5% normal donkey serum for 30 min each. The coverslips were washed in PBS and incubated for 1 h at 37°C with either a 1:1,000 dilution of preimmune serum or anti-BZP IgG at 10 μg/ml in PBS containing 3% BSA and 0.1% Triton X-100. After three washes in PBS for 15 min each, the coverslips were incubated with a biotinylated donkey anti-rabbit secondary antibody (Jackson ImmunoResearch) at ~10 μg/ml in PBS containing 3% BSA and 0.1% Triton X-100 for 1 h. Following three 15-min washes in PBS, a 1:100 dilution of streptavidin-linked Texas red (Jackson ImmunoResearch) was added to the coverslips for 45 min; after being washed in PBS–0.1% Triton X-100 three times for 15 min each, the cells were mounted in Aqua-Poly/Mount (Polysciences, Inc.).

(iv) Tissue section immunostaining. Deparaffinized sections were permeabilized and blocked (24) and then incubated with either BZP peptide 1 or peptide 2 antiserum or the corresponding preimmune serum, each diluted 1:3,000 in PBS–1% BSA–0.1% Triton X-100. Some experiments involved the use of an IgG fraction of immune serum diluted 1:1,000. All primary antibody incubations were carried out in a humid chamber at 4°C for at least 12 h. After unbound primary antibody was washed away as described above, the sections were incubated with biotinylated donkey anti-rabbit secondary antibody (Jackson ImmunoResearch) at ~10 μg/ml for 1 h at 22°C. Finally, following a similar washing of the unbound secondary antibody, either ~10 μg of Z-avidin–fluorescein isothiocyanate (Zymed Laboratories) per ml or ~5 μg of Z-avidin–horseradish peroxidase (Zymed Laboratories) per ml was incubated with the sections for 30 to 60 min at 22°C. Tissue-bound peroxidase was then visualized by using 3-amino-9-ethylcarbazole (24). BZP and growth hormone (GH) were colocalized in the pituitary gland by using both rabbit BZP antisera and an affinity-purified goat anti-GH antibody (Scantibodies Laboratories) diluted 1:100 in 1% BSA–0.1% Triton X-100 in PBS. Somatotrope-bound antibodies to GH were visualized with donkey anti-goat-Texas red at a 1:100 dilution (ML grade; Jackson ImmunoResearch).

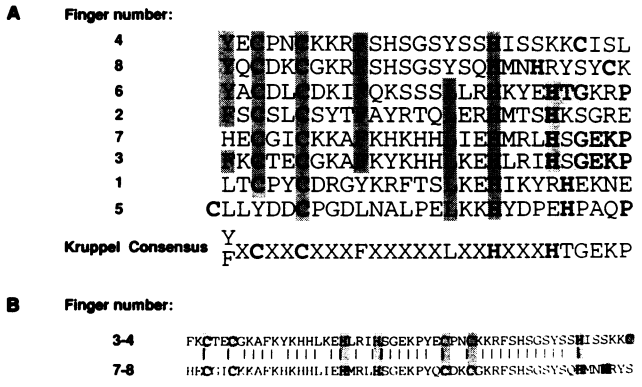

FIG. 3. (A) Comparison of the eight zinc finger motifs. Shaded areas indicate similarities with the Krüppel consensus (47). (B) Alignment of fingers 3 and 4 with fingers 7 and 8. Putative zinc ion-coordinating residues are shown in boldface.

(v) Control staining experiments. Specific BZP immunostaining was determined by incubation of adjacent sections of mouse tissues in the cognate preimmune serum and by comparing the staining patterns obtained with the two different BZP peptide antibodies. Controls for staining specificity in double-labeling experiments included sequential staining for each antigen with replacement of one primary antibody with nonimmune serum, reversal of staining order, and comparisons of single immunostaining experiments on adjacent serial sections. Results obtained from the combination of pGST-1 and pGST-2 IgG fractions were confirmed by separate incubations with the individual IgG fractions.

In situ hybridization. Mouse tissues were either fixed as described above and then mounted on Probe On-Plus microscope slides (Fisher Scientific) or flash frozen for 2 min in LN_2-cooled isopentane and then stored briefly on dry ice prior to transfer to the cryostat chamber. After equilibration of the tissue to cryostat temperatures (~−30°C), tissues blocks were embedded in OCT (Miles Scientific) and sectioned at 6 μm. Sections were briefly melted onto autoclaved Probe On-Plus slides, fixed in ice-cold 4% paraformaldehyde in PBS for 10 min, washed in PBS, quickly dehydrated through an ethanol series, and then air dried before storage in desiccant until hybridization.

RNA probe synthesis. ^{35}S-labeled sense and antisense RNA probes were synthesized from BZP clone 5 linearized with either *Kpn*I or *Bam*HI for in vitro transcription of sense or antisense cRNA probes, respectively, using [^{35}S]UTP (800 Ci/mmol; New England Nuclear) and T3 or T7 RNA polymerase. Following DNase I digestion, the probe was hydrolyzed to ~100 to 150 nucleotides (20), neutralized, and ethanol precipitated with 10 mg of glycogen per ml. The RNA probes were resuspended in 0.1 M dithiothreitol and stored at −20°C until used. Prehybridization, hybridization, and posthybridization steps were as described previously (23). Some slides were counterstained with either 0.002% toluidine blue or ~5 μg of bisbenzimide (Hoechst 33342; Polysciences) per ml.

Microscopy and photography. Micrographs were recorded on Kodak T-Max 100 film, with single exposures of FITC and Texas red fluorescence taken at ASA settings of 400 and 500, respectively, and transmitted light-dark-field images taken at ASA 100 to 160, using a Leitz Laborlux S with integrated automatic exposure metering and appropriate filter cubes for

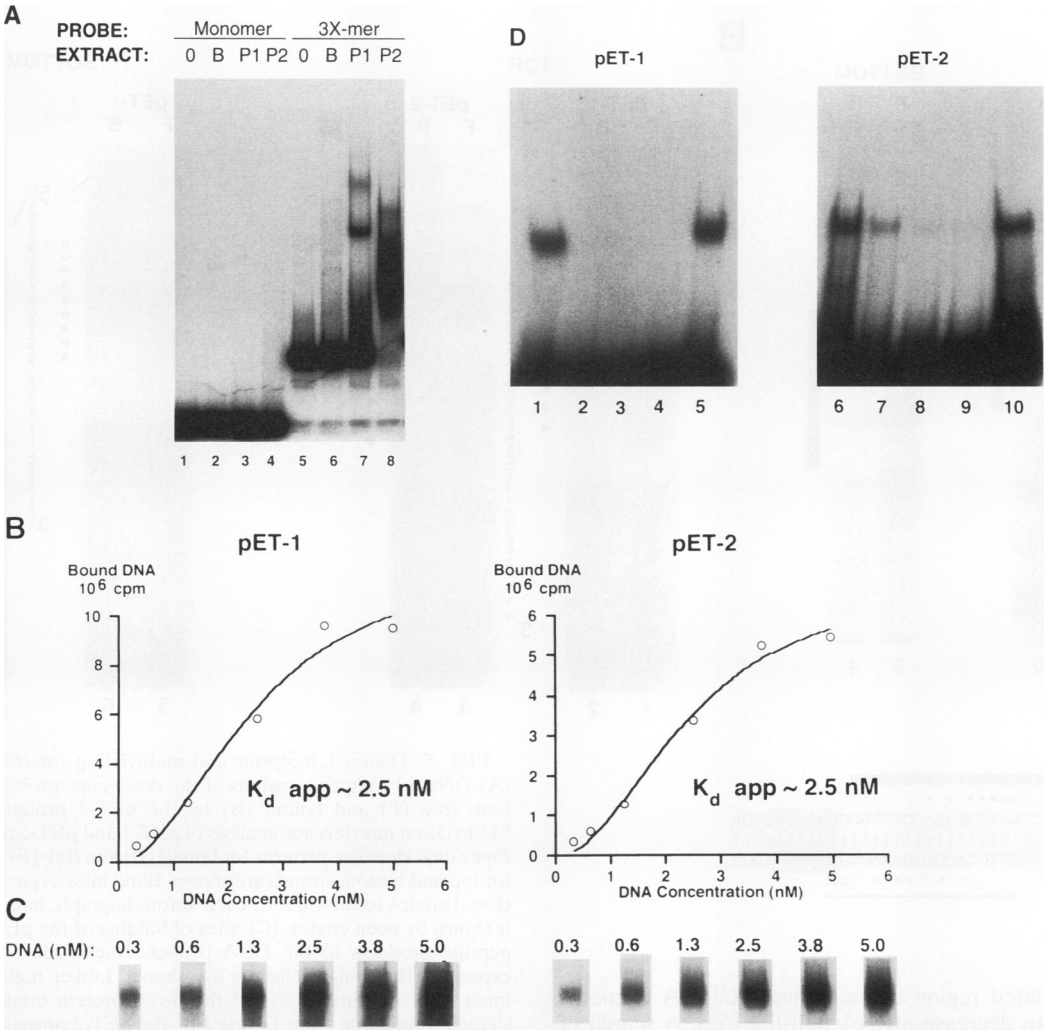

FIG. 4. DNA binding by BZP peptides. (A) Gel mobility shift assay analysis of DNA binding by partially purified pET-1 and pET-2 protein products. One copy (lanes 1 to 4) or three copies (lanes 5 to 8) of the annealed oligonucleotide pair used to screen the library were end labeled with ^{32}P and used in mobility shift reaction mixtures containing no protein (0), 30 μg of nontransformed *E. coli* extract (B), 1 μg of partially purified pET-1 product (P1), or 1 μg of partially purified pET-2 product (P2). The reaction mixtures were fractionated on a 4% nondenaturing gel, and the autoradiograph shown was obtained. (B) DNA binding affinity of pET-1 and -2 peptides. Gel mobility shift assays were performed with the pET-1 and -2 peptides and various concentrations of the three-copy probe. The bound counts were determined and plotted against the total DNA concentration. Fifty percent maximal binding was taken as the apparent K_d and was ~2.5 nM for both pET-1 and pET-2. (C) Autoradiograph of mobility shifts from which the plots in panel B were obtained. (D) Competition analysis. Both pET-1 (100 ng) and pET-2 (40 ng) were preincubated alone (lanes 1 and 6) or with a 25-fold molar excess of several unlabeled DNA competitors: an oligonucleotide pair with three copies of the binding site (lanes 2 and 7), an oligonucleotide pair containing three copies of the 9-bp BZP element (lanes 3 and 8), the concatemerized DNA used in the original library screen (lanes 4 and 9), and a concatemerized but unrelated oligonucleotide pair (lanes 5 and 10). Protein binding to DNA was specifically competed for only with DNA fragments containing multiple copies of the 9-bp binding site.

FITC, Texas red, and UV excitation. Bright-field images of the immunoperoxidase experiments were enhanced with a 550-nm interference filter. HIT cell immunofluorescence was imaged with a Zeiss 410 laser scanning confocal microscope and the 543-nm line of a HeNe laser and then formatted in Aldus Persuasion (version 2.1) on a Macintosh Quadra 700.

Nucleotide sequence accession number. The GenBank accession number of BZP is L13856.

RESULTS

Cloning and characterization of BZP. Two HIT cell cDNA expression libraries were screened with a multimerized double-stranded DNA probe containing upstream glucokinase promoter sequences by the method of Singh et al. (54). The monomeric probe contained a 6-bp target element, UPE-2, that binds a ~50-kDa pancreatic β-cell-specific protein in both mobility shift and UV cross-linking assays (53). Four independent cDNA clones were identified from the libraries whose fusion gene products bound to the multimerized probe. Analysis of these DNAs showed they were derived from a single mRNA of 5,098 bp that encoded a protein of 114 kDa (1,043 amino acids) from an open reading frame of 3,131 bp (Fig. 1). The putative translation initiation codon at base 123 (CCAG CATGC) conforms to the Kozak consensus sequence (29). A polyadenylation signal is located upstream of the poly(A) tail.

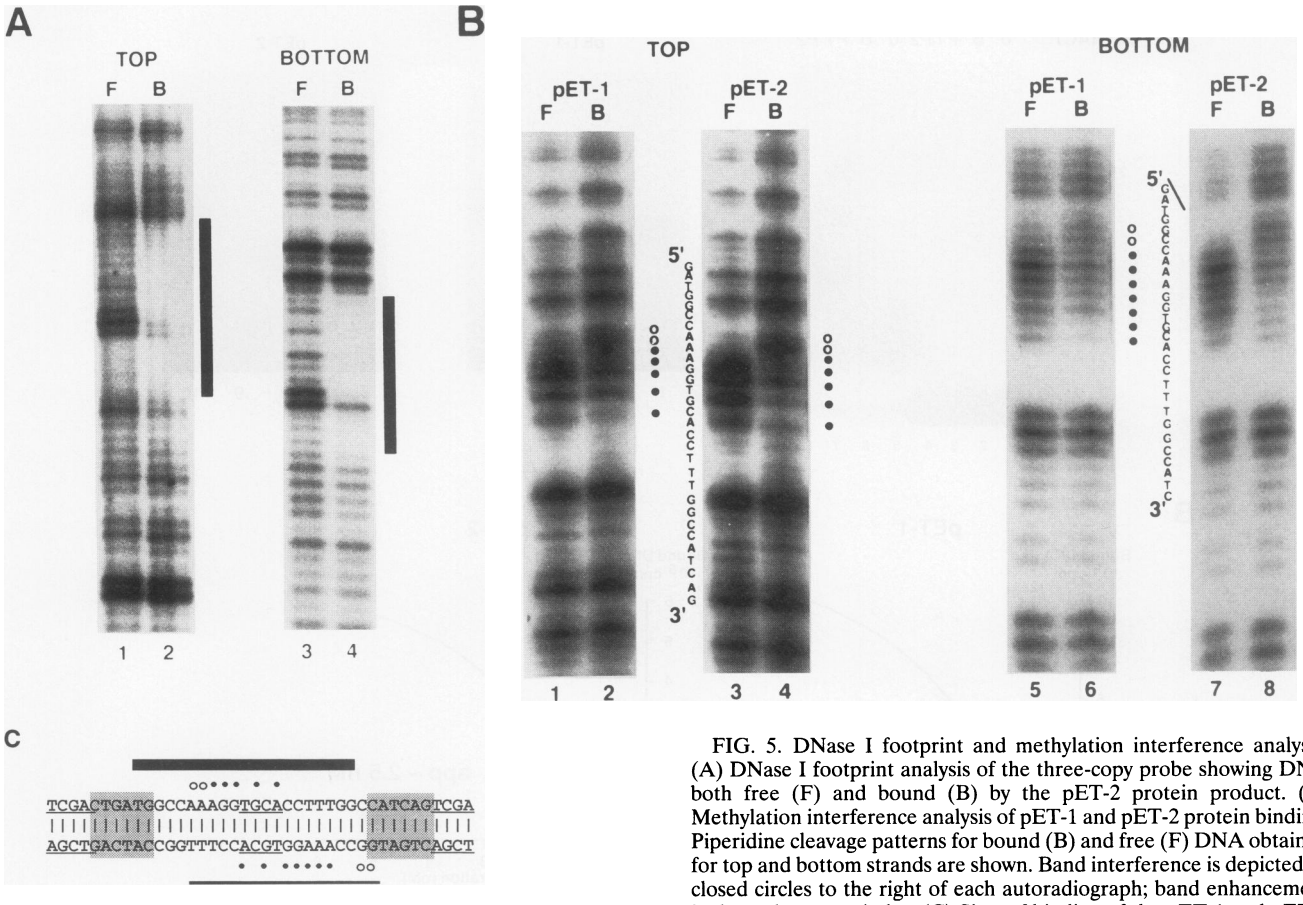

FIG. 5. DNase I footprint and methylation interference analysis. (A) DNase I footprint analysis of the three-copy probe showing DNA both free (F) and bound (B) by the pET-2 protein product. (B) Methylation interference analysis of pET-1 and pET-2 protein binding. Piperidine cleavage patterns for bound (B) and free (F) DNA obtained for top and bottom strands are shown. Band interference is depicted by closed circles to the right of each autoradiograph; band enhancement is shown by open circles. (C) Sites of binding of the pET-1 and pET-2 peptide products to the DNA probes. Nucleotide contacts for the expressed BZP finger clusters are shown. Linker regions are underlined, and the binding site of the β-cell protein originally sought is shaded. Protection from DNase I by the pET-2 protein is shown by a darkened bar. Closed circles indicate band diminishment, and open circles denote band enhancement.

The 3′ untranslated region contains five AUUUA elements which may act to decrease mRNA half-life (52). A search of GenBank (version 70) indicated that the sequence was novel; thus, we named the encoded protein BZP.

BZP was larger than the 50-kDa UPE-binding protein sought and, as shown below, did not bind to the intended target element in the probe. However, the protein had several interesting features that led us to study it further. Both the amino- and carboxy-terminal ends are highly acidic; 28 of the first 94 residues and 58 of the last 140 residues are negatively charged at a neutral pH, contributing to an overall acidic pK_a of ~4.8 for the entire molecule. Seven of the eight zinc finger motifs in BZP are grouped in clusters of four and three fingers that are located near the amino- and carboxy-terminal ends of the molecule, respectively. A single finger motif is located near the center of the molecule (Fig. 1 and 2). The finger motifs generally conform to the Krüppel consensus of $CX_2CX_3FX_5LX_2HX_3H$ (Fig. 3A) (50). Every finger contains 12 amino acids between the amino- and carboxy-terminal zinc-coordinating residues, and all have either a phenylalanine at position 4 or a leucine at position 10. The last two finger motifs in each cluster possess a 63% amino acid identity (34 of 54 residues; Fig. 3B). BZP also contains multiple potential phosphorylation sites throughout its sequence (25). Seven consensus sites for protein kinase C and eight putative sites for cyclic AMP-dependent protein kinase were identified (not shown), most of which are located nearby or within zinc finger motifs. Additionally, there are 30 consensus phosphorylation sites for casein kinase II and three consensus sites for $p34^{cdc2}$ kinase (not shown).

Expression of BZP peptides. To characterize the DNA binding specificity of BZP and to generate antibodies against the protein, four different peptides were expressed in *E. coli* as shown in Fig. 1B. The amino- and carboxy-terminal zinc finger clusters were expressed by using pET15b, a vector that adds a six-histidine repeat to the amino terminus (pET-1 and pET-2 in Fig. 1B), thereby enabling purification by nickel-agarose affinity chromatography. Full-length BZP was not efficiently expressed in *E. coli* by using pET15b and could be detected only by immunoblot analysis using antisera generated against the fusion peptide products of pGST-1 and pGST-2 (Fig. 1B). However, the observed size of ~175 kDa was anomalously large, consistent with a pattern of lower than expected migrations observed with several other large zinc finger proteins (32, 44, 49, 51).

Analysis of BZP peptide DNA binding. In preliminary studies using a Southwestern (DNA-protein) blotting method, both the amino- and carboxy-terminal finger clusters bound to the multimerized DNA probe, whereas neither bound to a monomeric probe (not shown). Therefore, to clarify the DNA binding specificity of the BZP finger clusters, both a single-copy and a three-copy cloned multimer of the oligonucleotide pair were tested for DNA binding in a mobility shift assay using

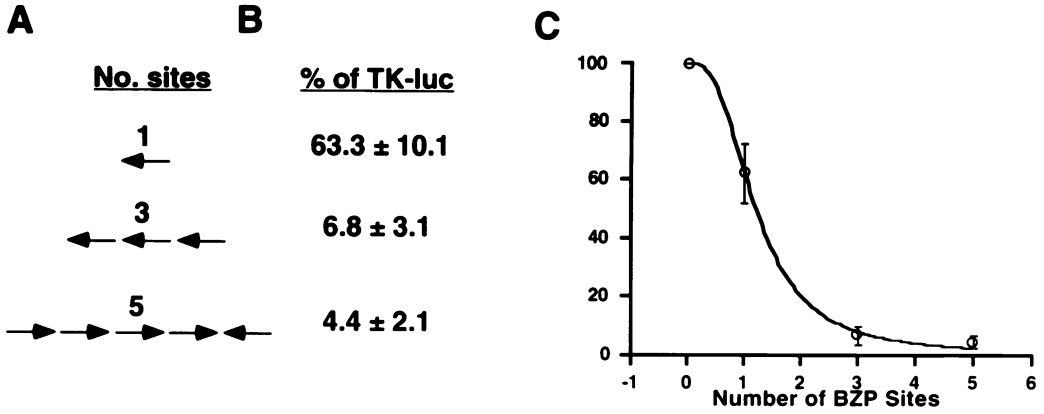

FIG. 6. Copy-dependent transcriptional repression of a heterologous promoter. The number and orientation of BZP binding sites (A) and their effects on transcription of a TK-luc fusion gene in HIT M2.2.2 cells (B and C) are shown. Transcriptional activity is shown as a percentage of the normalized luciferase activity observed for the plasmid (pTK-luc) without any sites. The datum points were fit to a sigmoidal curve.

the purified peptides containing the amino- or carboxy-terminal finger motifs. Neither peptide bound the monomeric probe, but both bound the multimerized probe (Fig. 4A). Limiting dilution of the target DNA sequence in the presence of a fixed amount of protein (Fig. 4B and C) determined an apparent K_d of 2.5 nM for the interaction between each finger cluster and the target sequence. Diminished binding of the BZP peptides to DNA was observed after preincubation with a 25-fold excess of three different cold specific competitor DNA fragments. However, competition was not observed with two DNA fragments containing mutated BZP binding sequences (Fig. 4D), suggesting that DNA recognition by both zinc finger cluster peptides was sequence specific.

DNase I footprinting and methylation interference analysis were performed to further characterize DNA binding by the amino- and carboxy-terminal finger clusters. The carboxy-terminal finger peptide showed a footprint of 15 and 20 bases on the bottom and top DNA strands of the multimerized DNA probe, respectively (Fig. 5A and C). The higher resolution provided by the methylation interference analysis allowed comparison of the actual nucleotide contacts made by the two finger clusters. Both diminution and enhancement of bands corresponding to multiple adenines and guanines on both strands within this palindromic region were seen (Fig. 5B and C). Similar contact sites were observed on both strands of the probe for both finger clusters. However, the intensity of interference varied at positions within the contacted region, possibly reflecting the relative importance of specific bases for protein binding. While the dual and overlapping 9-bp contact sites within the probe precluded an exact determination of base interactions, base contacts were observed within the 9-base AAAGGTGCAA sequence present on both the top and bottom strands (Fig. 5C). These interactions occurred within the region of the DNase I footprint (darkened bars). The BZP binding sites in this probe were distinct from UPE-2 (53).

Transcriptional repression by BZP. Transient transfection assays were used to determine whether the 9-bp element identified above was able to affect transcription of a *cis*-linked promoter. When one, three, and five copies of the AAAGGT GCA sequence were inserted upstream of a minimal herpes simplex virus thymidine kinase promoter, transcription was

TABLE 1. Effect of cotransfecting a BZP expression vector with the TK-luc or 3X-TK-luc gene

Cell line (*n*)	Expression plasmid	Luciferase gene expression (normalized relative light units)	
		TK-luc	3X-TK-luc
HIT M2.2.2 (4)	pCMV4	88,157	3,568
	pCMV-BZP	69,997	1,701
P		>0.01	0.0001
NIH 3T3 (6)	pCMV4	299,019	21,768
	pCMV-BZP	417,890	5,979
P		>0.01	0.000002

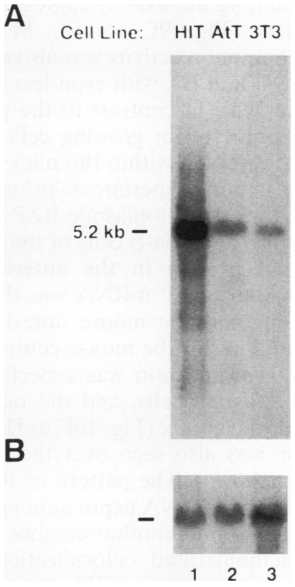

FIG. 7. Northern analysis of BZP mRNA. (A) BZP mRNA. (B) Actin mRNA control after the BZP probe was washed from the blot. Each lane contained 10 μg of poly(A)$^+$ RNA from HIT M2.2.2 (hamster β-cell origin; lane 1), AtT-20 (mouse corticotrope origin; lane 2), or NIH 3T3 (mouse fibroblast origin; lane 3) cells. The membrane was probed with a radiolabeled ~1,900-bp *Pst*I-*Pst*I fragment of BZP cDNA clone 5, nucleotides 1 to 1882, and the autoradiographs obtained are shown.

inhibited by 37, 93, and 96%, respectively (Fig. 6). Cotransfection of pCMV-BZP with the TK-luc gene containing three BZP binding sites (3X-TK-luc) reduced transcription even further in both HIT M2.2.2 and NIH 3T3 cells (Table 1). Cotransfection of pCMV-BZP resulted in a greater repression in NIH 3T3 cells than in HIT cells, 73 versus 52%, possibly reflecting the greater amount of endogenous BZP in HIT cells, as was observed by immunoblot analysis (see Fig. 8).

BZP mRNA and immunoreactivity in cell lines. Northern (RNA) blot analysis identified a BZP mRNA of ~5.2 kb in NIH 3T3, AtT-20, and HIT M2.2.2 cells, with the last cell type showing a severalfold enrichment (Fig. 7). Immunoblot analysis of nuclear extracts from these same cell lines by using immune serum detected a protein of ~185 kDa (Fig. 8) that was not seen when the preimmune serum was used (not shown). BZP protein also appeared to be enriched severalfold in HIT M2.2.2 cells compared with NIH 3T3 cells (Fig. 8). The reason for the ~10-kDa discrepancy in the size of BZP between the native and *E. coli*-expressed protein is not known but may be due to posttranslational modifications that occur in eucaryotic cells. BZP was also identified by immunohistochemistry in HIT M2.2.2, AtT-20, NIH 3T3, βTC-3, αTC-6, and H4IIE cells (not shown), in which it was consistently nuclear in location.

BZP mRNA and protein in the pancreatic islet. Hybridization of adult mouse pancreatic sections with antisense ^{35}S-labeled BZP RNA probes showed silver grains over the islets that were not seen with the sense-strand probe (Fig. 9A and B). The signal was distributed uniformly throughout the islet, suggesting that all endocrine cell types of the islet express BZP mRNA. A considerably weaker hybridization signal was observed over the epithelium of the pancreatic ducts (not shown). IgG fractions of both BZP antisera (anti-pGST-1 and -2) showed specific BZP immunoreactivity in the endocrine pancreas of a neonatal mouse (Fig. 9C to H) that was predominately cytoplasmic in location. The strongest BZP immunoreactivity was seen among the loosely aggregated cells of 1-day-old neonatal islets (Fig. 9C to F). Moderately intense cytoplasmic BZP immunoreactivity was also observed in 4-day-old animals (Fig. 9G and H), with even less signal detected in adult mice (not shown). In contrast to the pattern of subcellular localization observed in growing cells in culture, BZP protein was never observed within the nuclei of mouse or rat islet cells. Double-staining experiments using anti-insulin antibodies confirmed that the cytoplasmic BZP immunoreactivity was present in both β and non-β cells of the islet (not shown).

BZP mRNA and protein in the anterior pituitary and central nervous system. BZP mRNA was detected by in situ hybridization throughout the mouse anterior pituitary (Fig. 10A and B) and in areas of the mouse central nervous system (Fig. 10F to H). Hybridization was especially strong in the hypothalamus, ependymal cells, and the outer granular and pyramidal layers of the cortex (Fig. 10F to H). Equally intense BZP hybridization was also seen over the hippocampus and cingulate gyri (not shown). The pattern of BZP immunoreactivity roughly paralleled mRNA expression in the pituitary and brain. Double-labeling immunofluorescence assays in the anterior pituitary demonstrated colocalization of cytoplasmic BZP protein and immunoreactive GH among the somatotrope population (Fig. 10C to E). Although double-labeling experiments with other anterior pituitary cell markers were not undertaken, BZP immunoreactivity was notably absent in many cells without GH immunoreactivity. In the neonate central nervous system, BZP immunoreactivity was widespread among neutral cells (Fig. 10F, G, and I to L). BZP protein was found in the proliferative ependymal cell layer of the neonate brain and in the nuclei of neural cells in the nearby parenchyma (Fig. 10I and J). Nuclear BZP immunoreactivity was observed with varying intensities among scattered cells throughout the brain and spinal cord of the adult, in a more widely dispersed pattern than in the neonate (Fig. 10K to M).

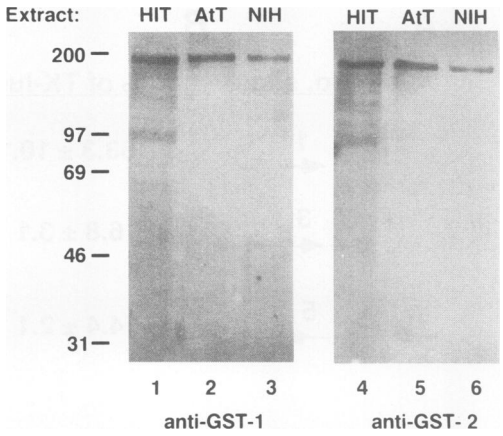

FIG. 8. Immunoblot analysis of protein. The IgG fractions of two different anti-GST-BZP antisera each detect a protein in nuclear extracts from three cell lines. Thirteen micrograms of nuclear extract from HIT M2.2.2 (hamster β-cell origin; lanes 1 and 4), AtT-20 (mouse corticotrope origin; lanes 2 and 5), or NIH 3T3 (mouse fibroblast origin; lanes 3 and 6) cells was fractionated by SDS-PAGE (7.5% gel). Proteins were transferred to Immobilon P and probed with the indicated IgG. Positions of molecular mass standards (in kilodaltons) are shown on the left.

BZP mRNA and protein in other locations. Nuclear BZP immunoreactivity was also observed among mesenchymal cells, intestinal crypt cells, and smooth muscle cells of the neonate gut as well as the germinal cells of the dental papilla (not shown). BZP gene expression in crypt cells of the intestine was further substantiated by in situ hybridization (not shown). Neither BZP mRNA nor immunoreactivity was detected in adult mouse lung, liver, spleen, kidney, skeletal muscle, and heart tissues or in most other tissues of neonates.

Change in the subcellular localization of BZP by serum starvation. Because of the difference in the subcellular localization of BZP immunoreactivity between cells growing in culture and their parent tissues, the effect of serum deprivation on subcellular localization of BZP in HIT M2.2.2 cells was tested. Overnight serum starvation caused a partial and reversible shift of BZP immunoreactivity to the cytoplasm, often appearing as a ring of fluorescence surrounding the nuclear envelope (Fig. 11A). Serum replacement for 1, 3, or 6 h was unable to completely reverse the intracellular shift (not shown); however, BZP immunoreactivity returned to a predominately nuclear location after 18 h of serum refeeding (Fig. 11B). In addition to the immunocytochemical detection of BZP in cultured cells, BZP was also assessed by immunoblotting of nuclear and cytoplasmic cell extracts obtained after the same treatments. Cytosolic BZP immunoreactivity was detected only after serum deprivation (compare Fig. 11C and D), whereas nuclear BZP immunoreactivity increased with serum treatment. Lastly, the effect of serum deprivation on transcription of the TK-luc fusion gene was assessed. Transcription of the 3×-TK-luc gene was enhanced by more than twofold in HIT M2.2.2 cells in the absence of serum (Table 2).

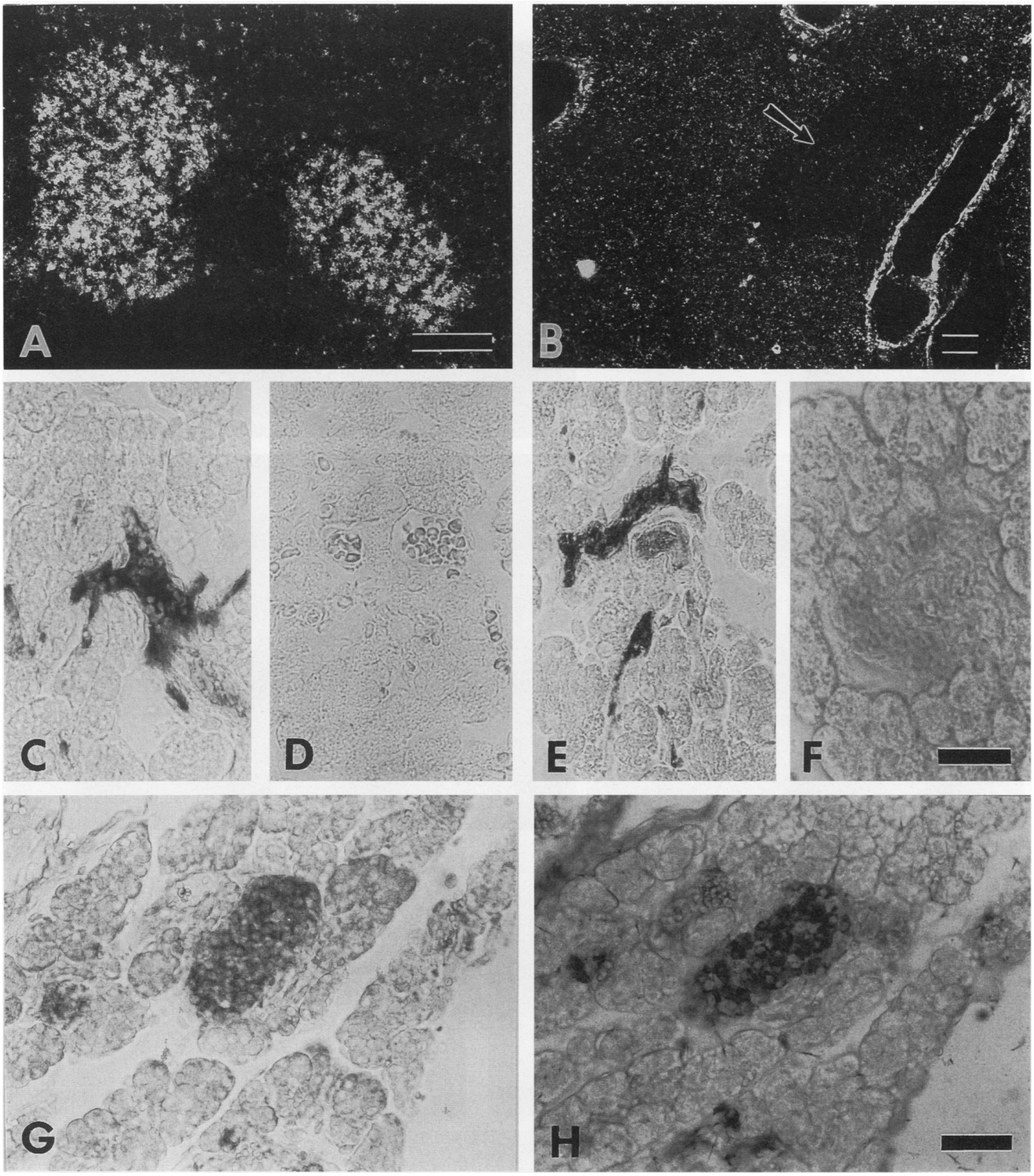

FIG. 9. Identification of BZP mRNA and protein in mouse pancreatic islets. (A) Dark-field photomicroscopy following in situ hybridization of an antisense BZP RNA probe to cryosectioned adult mouse pancreas. Silver grains are observed over islet cells but not exocrine pancreas. (B) Section similar to that in panel A but with a sense-strand BZP RNA probe. No silver grains are seen over a large islet (arrow). (C to F) Immunocytochemical localization of BZP in islets of 1-day-old neonates, using nonadjacent sections of the same islet region. (C) Strong cytoplasmic immunoperoxidase staining obtained with BZP peptide 1 antibody in a developing islet. (D) Comparable field of the same islet incubated with the preimmune serum for anti-BZP peptide 1. (E) Immunoperoxidase staining of the same islet incubated with anti-BZP peptide 2. A cytoplasmic staining pattern among islet cells similar to that in panel C is seen. (F) Comparable field of the same islet incubated with the preimmune serum for anti-BZP peptide 2. (G and H) Immunocytochemical localization of BZP in islets of 4-day-old mice. (G) Immunoperoxidase staining for BZP peptide 1 showing moderate staining of islet cell cytoplasm. (H) Adjacent section of pancreas stained for BZP peptide 2 revealing a staining pattern similar to that in panel G. Double-immunofluorescence experiments with anti-insulin antibodies were performed to confirm location of BZP immunoreactivity in islet endocrine cells (not shown). All scale bars are equal to 50 μm.

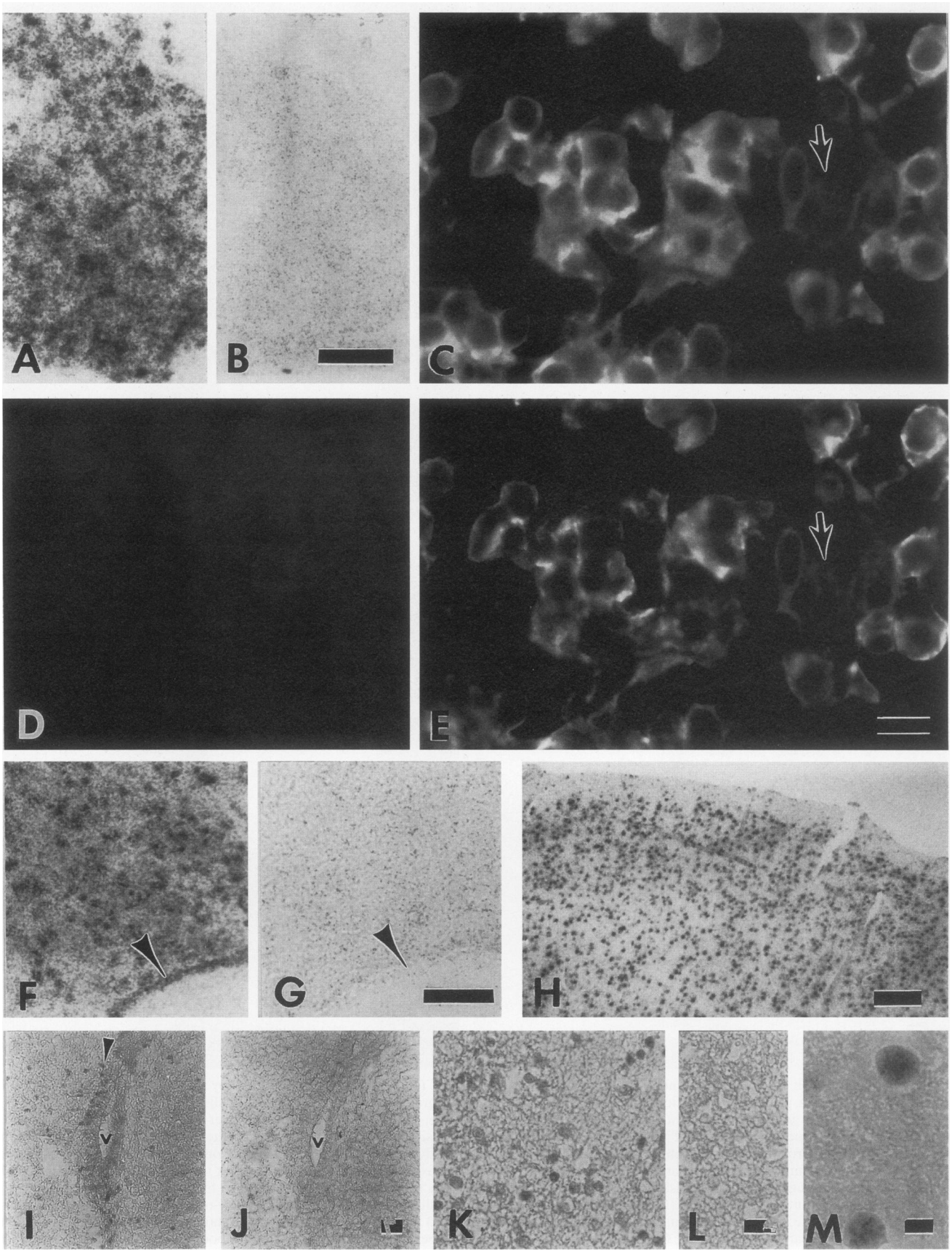
A
B
C
D
E
F
G
H
I
J
K
L
M

FIG. 10. Localization of BZP mRNA and protein in the mouse anterior pituitary gland and central nervous system. (A) In situ hybridization of an antisense BZP RNA probe to a section of adult mouse pituitary sagittal sections through the pars distalis. Hybridization signal is observed over the anterior pituitary but not the posterior lobe (not shown). Scale bar equals 50 μm. (B) Section adjacent to that in panel A hybridized to a sense BZP probe showing the lack of a hybridization signal. Scale bar equals 50 μm. (C to E) Immunofluorescence staining using anti-BZP peptide 2 and anti-GH antibodies in the anterior pituitary. (C) Cytoplasmic BZP immunoreactivity is observed among many cells of the anterior pituitary with some cells lacking fluorescence (arrow). (D) Section adjacent to that in panel C incubated with the preimmune serum for the BZP peptide 2 antibody. (E) Same section as in panel C stained for GH to identify somatotropes. BZP immunoreactivity is observed predominately in somatotropes, as some minor pituitary cell types lack both BZP and GH immunoreactivity (arrow). Scale bar equals 10 μm. BZP peptide 1 antiserum was also found to react with a cytoplasmic component of somatotropes (not shown). (F) In situ hybridization of an antisense BZP RNA probe to the hypothalamic region of an adult mouse showing silver grains over the parenchyma and the ependymal cell layer lining the third ventricle (arrowhead). (G) Section adjacent to that in panel F incubated with a sense BZP probe showing the lack of hybridization to ependymal cells (arrowhead). Scale bars represents 50 μm. (H) Overview of section of cerebral cortex that was hybridized with an antisense BZP RNA probe revealing a strong hybridization signal over cells in the outer granular and pyramidal layers. A strong hybridization signal was also observed over cells of the hippocampal and cingulate gyri (not shown). Scale bar equals 200 μm. (I) Immunoperoxidase staining for BZP in the neonate brain. Low levels of immunoreactivity among the germinal ependymal layer and moderate levels of immunoreactivity within the nuclei of nearby cells were seen (arrows). (J) Adjacent section of neonate brain incubated with the corresponding preimmune serum demonstrating the lack of staining. V, ventricle. Scale bar represents 20 μm. (K) Nuclear BZP immunoreactivity among scattered cells in the neonate spinal cord. (L) Adjacent section of neonate spinal cord incubated with the corresponding preimmune serum. Scale bar equals 20 μm. (M) High-power field of adult mouse brain stained with BZP antibody showing strong nuclear immunostaining. Scale bar equals 5 μm.

DISCUSSION

Cloning of a novel zinc finger protein. In an attempt to clone a factor of ~50 kDa that is expressed in pancreatic β cells, we instead obtained cDNAs encoding a novel 114-kDa zinc finger protein that has been termed BZP. In large part, the cloning of BZP was due to the inadvertent creation of a binding motif for this protein by multimerizing the probe. We have shown that BZP binds with high affinity to sequences that become juxtaposed only by ligation. cDNA expression cloning strategies are widely used to clone new DNA-binding proteins. Our experience illustrates the risk of creating new DNA-protein interactions by the multimerization of monomeric DNA probe sequences.

Structural similarity of BZP to other zinc finger proteins. BZP contains eight zinc finger motifs, seven of which are divided into two clusters at opposite ends of the molecule. Other zinc finger proteins that contain dispersed zinc finger motifs have been cloned; examples include the *Drosophila Hunchback*, *Teashirt*, and *Suvar(3)7* gene products and the vertebrate genes for PRDII-BF1, Evi-1, and Zn-15. Hunchback contains six zinc finger motifs arranged into two clusters of four and two fingers (60). Teashirt (13) and Suvar(3)7 (45) contain three and five finger motifs, respectively, that are individually dispersed. Zn-15 is named for its 15 zinc finger motifs, 12 of which are loosely arranged into two clusters of six each (32). Of these examples, PRDII-BF1 is structurally the most similar to BZP. This molecule contains five finger motifs, four of which are arranged into two structurally related pairs that lie near opposite ends of the 298-kDa molecule (12). A single, isolated finger is also located near the center of the protein.

Function of BZP. The cloning of BZP in the manner described did not allow its function to be studied in the context of a natural target gene since none are known. However, when elements to which BZP binds were linked in *cis* to the thymidine kinase promoter, an inhibitory effect was observed. Thus, at least in the context examined, BZP appears to act as a transcriptional repressor. Whether BZP has the same effect on natural target genes remains to be determined. Other zinc finger proteins have well-documented effects on gene transcription, with most having been found to augment rather than inhibit transcription. For instance, Zn-15 synergistically activates transcription of the GH gene in combination with Pit-1 (32), whereas PRDII-BF1 and Evi-1 stimulate transcription in a serum-dependent manner (12, 35). Whether BZP has a role in development, as is the case for the *Drosophila* zinc finger proteins Hunchback (31) and Teashirt (13), is not yet known.

DNA sequence recognition by BZP. The amino- and carboxy-terminal finger clusters of BZP demonstrated similar DNA binding specificities and affinities, as examined by gel mobility shift and methylation interference assays. Thus, given the high degree of primary amino acid sequence identity between finger motifs 3 and 4 and finger motifs 7 and 8, these two finger pairs may be the main determinants of DNA sequence recognition by this protein. A similar degree of sequence similarity exists for the amino- and carboxy-terminal zinc finger pairs of PRDII-BF1, which are also able to bind to the same DNA sequence (12). The multimerized DNA probe used to screen the HIT cell libraries contained two overlapping 9-bp binding sites for BZP (Fig. 6C). Crystallographic and mutagenic studies have shown that C_2H_2 zinc fingers can interact with one to five bases of DNA, although it appears that many interact with three bases (36, 39, 40). Binding to a 9-bp element is, therefore, consistent with base contacts from two or three zinc fingers, as appears to be the case with BZP, but whether this is the minimum or optimum sequence for binding remains to be determined. It is not known if the fourth finger in the amino-terminal cluster, or the fifth isolated finger near the middle of BZP, is also involved in DNA binding. Some zinc fingers do not interact with DNA at all but may instead be involved in protein-protein contacts (40).

The significance of the distances between the zinc finger motifs in BZP is not known, but the BZP finger clusters themselves contain many of the exceptions that are associated with jumper-linker recognition of DNA (28). Finger motifs that contain more than three residues between carboxy-terminal zinc-complexing histidine residues, followed by a hydrophobic or large interfinger linker region, may contact adjacent bases on opposite strands of DNA (28). Some other factors with widely dispersed zinc finger motifs, e.g., PRDII-BF1, Zn-15, Suvar(3)7, Hunchback, and Teashirt, also contain more than three residues between their carboxy-terminal zinc-complexing amino acids, suggesting that overall structural similarity may reflect common modes of DNA recognition. The duplicated finger motifs in BZP also suggest that there may be a variety of natural target sites for DNA binding by this protein, perhaps some that contain complex target elements with intervening bases that are not involved in DNA-protein contacts. Alternately, it is possible that DNA binding by only one of the two sets of zinc finger motifs is sufficient for

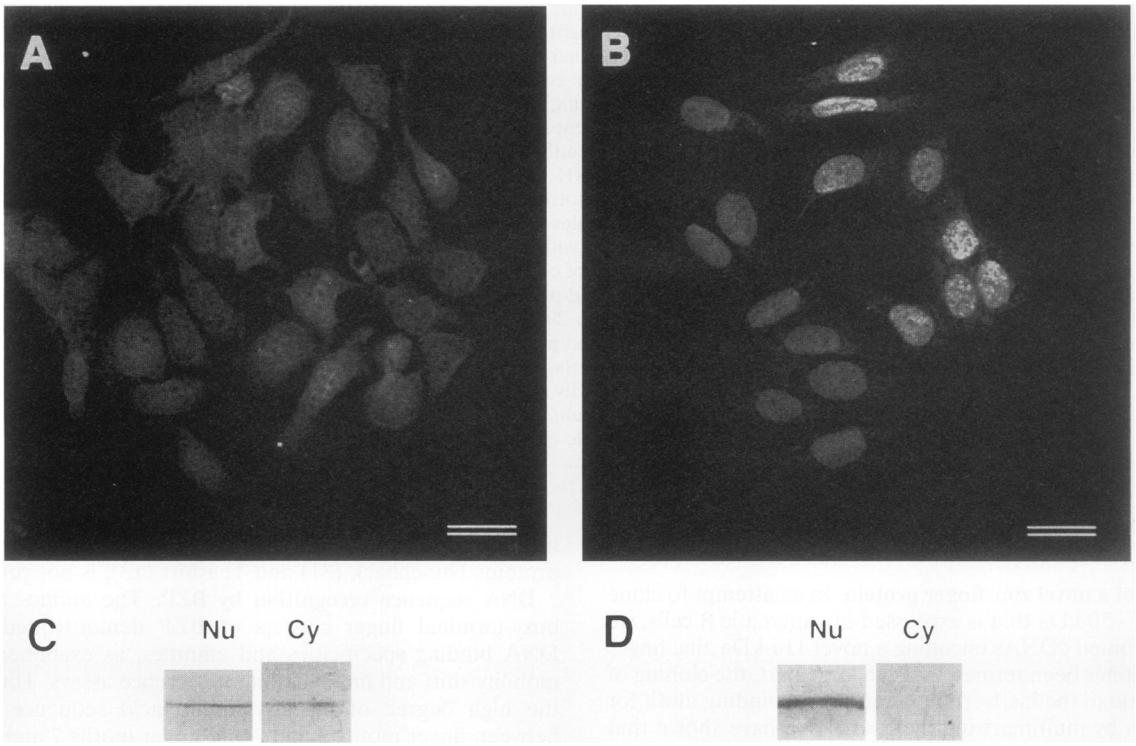

FIG. 11. Effect of serum on subcellular localization in HIT M2.2.2 cells. (A and B) HIT M2.2.2 cells after incubation in the absence (A) or presence (B) of 15% equine serum–2% fetal bovine serum for 18 h. Immunohistochemistry was performed by incubation with an equivolume mixture of anti-GST-BZP antibodies followed by incubation with a biotinylated donkey anti-rabbit secondary antibody and streptavidin-linked Texas red and visualized by laser scanning confocal microscopy. Scale bars, 10 μm. (C) BZP immunoblot obtained by using antibody 2 of HIT M2.2.2 cell nuclear (Nu) and cytoplasmic (Cy) extracts after 18 h of serum deprivation, as for panels A and B. (D) BZP immunoblot obtained by using antibody 2 of HIT M2.2.2 cell extracts after 18 h of serum treatment. For panels C and D, only the BZP-immunoreactive band at ~185 kDa is shown. Similar results were obtained with antibody 1 (not shown).

interaction at a target gene. Thus, a variety of models for DNA binding by BZP remain plausible until several natural target genes have been identified and characterized.

Variable subcellular distribution of BZP. BZP mRNA and protein expression was identified in several tissues but was predominately located in pancreatic islets, anterior pituitary, and central nervous system. Pancreatic islets and anterior pituitary appear to be rich sources of BZP, although the protein is not restricted to neuroendocrine cells. Indeed, the pattern of BZP immunoreactivity in the neonatal and adult mouse central nervous system suggests a complex pattern of expression, both at the cellular level and at the subcellular level. It is particularly interesting that within different cell types, the subcellular location of BZP varies. BZP immunoreactivity was found within the nuclei of some mouse cells, although in the anterior pituitary, endocrine pancreas, and portions of the central nervous system, the protein was predominately cytoplasmic. This contrasts with its location in cultured cells growing in media supplemented with serum, in which case it is almost invariably located in the nucleus. The partial shift of BZP immunoreactivity to the cytoplasm after serum removal suggests that there are factors in serum that affect the subcellular location of this protein. The change in the subcellular location of BZP in response to a change in culture conditions is not unique, as the locations of the proto-oncogene c-*fos* and c-*myc* products and certain other cell cycle-dependent proteins such as proliferating cell nuclear antigen have been found to vary in a similar manner (64).

TABLE 2. Effect of serum on BZP inhibition of TK promoter activity[a]

Expression plasmid (*n*)	Luciferase gene expression (normalized relative light units)	
	TK-luc	3X-TK-luc
−Serum (4)	4,769 ± 1,150	974 ± 155
+Serum (4)	5,123 ± 306	444 ± 121
−/+ Ratio	0.93	2.13

[a] Ten micrograms of a TK-luc or 3X-TK-luc fusion gene was transfected into HIT M2.2.2 cells, and the cells were incubated for 24 to 36 h in the presence or absence of serum prior to harvest and measurement of luciferase activity.

The means by which BZP is sequestered in the cytoplasm has not been determined, but functional parallels with other cytoplasmically sequestered factors suggest that this may be a phosphorylation-mediated event. For instance, the subcellular distribution and function of the SV40 large T antigen are dependent upon phosphorylation of residues near the nuclear localization signal (22, 43, 46). Phosphorylation of T antigen by casein kinase II at a serine residue (number 2 in Fig. 12) enhances nuclear import (46), while $p34^{cdc2}$-mediated phosphorylation of a threonine residue (number 3 in Fig. 12) inhibits nuclear localization (22). A sequence similar to the nuclear localization signal of T antigen is found near the carboxy-terminal zinc finger cluster of BZP (Fig. 1 and 12). Rihs et al. have suggested that the nuclear localization of

```
                  1  23
SV40 Large T Antigen:  ADSQHSTPPKKK-RKVE
                       ||  ||||||| ||  |
BZP:                   NDS-DSTPPKKKTRKTE
```

FIG. 12. Similarity between region of BZP and SV40 T-antigen nuclear localization sequence. Sequences from BZP are aligned with those of the SV40 T-antigen nuclear localization signal. 1, 2, and 3 indicate the sites of phosphorylation by a double-stranded DNA-dependent protein kinase, casein kinase II, and $p34^{cdc2}$-dependent protein kinase, respectively, as described in the text.

proteins may be dependent upon a casein kinase II site-spacer-nuclear localization sequence motif (46) in which the casein kinase II phosphorylation site is located either 13 or 22 residues amino terminal to the nuclear localization signal. The presence of a potential casein kinase II phosphorylation site 15 residues amino terminal to the putative nuclear localization signal in BZP is consistent with the use of a similar phosphorylation-dependent nuclear localization mechanism.

Concluding comments. The variable subcellular compartmentalization of BZP in different cell types and the modulation of nuclear transport by serum suggest that there are complex regulatory mechanisms that control the translocation and function of this protein. However, whether BZP has a role in cellular growth and/or differentiation remains to be established. In any case, further studies to identify natural regulatory elements that bind this protein and the mechanisms that control its location in the cell appear warranted.

ACKNOWLEDGMENTS

These studies were supported by grants from the Juvenile Diabetes Foundation and the Public Health Service (DK42612 and DK42502).

We thank L. Moss, L. Sealy, and R. Stein for reagents; G. Robinson, J. Ozer, and B. Morris for helpful discussions or suggestions about the manuscript; and E. Zimmerman for technical assistance.

REFERENCES

1. **Anderson, K. V.** 1989. Drosophila: the maternal contribution, p. 1–37. *In* D. M. Glover and B. D. Hanes (ed.), Genes and embryos. IRL Press, Oxford.
2. **Andersson, S., D. N. Davis, H. Dahlback, H. Jornvall, and D. W. Russell.** 1989. Cloning, structure and expression of the mitochondrial cytochrome P-450 steroid 26-hydroxylase, a bile acid biosynthetic enzyme. J. Biol. Chem. **264**:8222–8229.
3. **Beg, A. A., S. M. Ruben, R. I. Scheinman, S. Haskill, C. A. Rosen, and A. S. Baldwin, Jr.** 1992. IκB interacts with the nuclear localization sequences of the subunits of NF-κB: a mechanism for cytoplasmic retention. Genes Dev. **6**:1899–1913.
4. **Berg, J. M.** 1990. Zinc fingers and other metal-binding domains. J. Biol. Chem. **265**:6513–6516.
5. **Brown, R. S., C. Sander, and P. Argos.** 1985. The primary structure of transcription factor TFIIIA has 12 consecutive repeats. FEBS Lett. **186**:271–274.
6. **Chavrier, P., P. Lemaire, O. Revelant, R. Bravo, and P. Charnay.** 1988. Characterization of a mouse multigene family that encodes zinc finger structures. Mol. Cell. Biol. **8**:1319–1326.
7. **Chavrier, P., M. Zerial, P. Lemaire, J. Almendral, R. Bravo, and P. Charnay.** 1988. A gene encoding a protein with zinc fingers is activated during G0/G1 transition in cultured cells. EMBO J. **7**:29–35.
8. **Chomczynski, P., and N. Sacchi.** 1987. Single-step method of RNA isolation by acid guanidinium thiocyanate-phenol-chloroform extraction. Anal. Biochem. **162**:156–159.
9. **Diakun, G. P., L. Fairall, and A. Klug.** 1986. EXFAS study of the zinc-binding sites in the protein transcription factor IIIA. Nature (London) **324**:698–699.
10. **Dohrmann, P. R., G. Butler, K. Tamai, S. Dorland, J. R. Greene, D. J. Thiele, and D. J. Stillman.** 1992. Parallel pathways of gene regulation: homologous regulators *SW15* and *ACE2* differentially control transcription of *HO* and chitinase. Genes Dev. **6**:93–104.
11. **Evans, R. M., and S. M. Hollenberg.** 1988. Zinc fingers: gilt by association. Cell **52**:1–3.
12. **Fan, C.-M., and T. Maniatis.** 1990. A DNA-binding protein containing two widely separated zinc finger motifs that recognize the same DNA sequence. Genes Dev. **4**:29–42.
13. **Fasano, L., L. Roder, N. Core, E. Alexandre, C. Vola, J. Jacq, and S. Kerridge.** 1991. The gene *teashirt* is required for the developmental of *Drosophila* trunk segments and encodes a protein with widely spaced zinc finger motifs. Cell **64**:63–79.
14. **Geisler, R., A. Bergman, Y. Hiromi, and C. Nusslein-Volhard.** 1992. *cactus*, a gene involved in dorsoventral pattern formation of Drosophila, is related to the IκB gene family of vertebrates. Cell **71**:613–621.
15. **Gessler, M., A. Poutska, W. K. Cavenee, R. L. Neve, S. H. Orkin, and G. A. P. Bruns.** 1990. Homozygous deletion in Wilms tumours of a zinc-finger gene identified by chromosome jumping. Nature (London) **343**:774–778.
16. **Ghosh, S., and D. Baltimore.** 1990. Activation in vitro of NF-κB by phosphorylation of its inhibitor IκB. Nature (London) **344**:678–682.
17. **Gilmore, T. D.** 1990. NF-κB, KBF-1, *dorsal*, and *rel*ated matters. Cell **62**:841–843.
18. **Giniger, E., S. M. Varnum, and M. Ptashne.** 1985. Specific DNA-binding of GAL4, a positive regulatory protein of yeast. Cell **40**:767–774.
19. **Harrison, S. C.** 1991. A structural taxonomy of DNA-binding proteins. Nature (London) **353**:715–719.
20. **Hartshorne, T. A., H. Blumberg, and E. T. Young.** 1986. Sequence homology of the yeast regulatory protein ADR1 with Xenopus transcription factor TFIIIA. Nature (London) **320**:283–287.
21. **Hunter, T., and M. Karin.** 1992. The regulation of transcription by phosphorylation. Cell **70**:377–387.
22. **Jans, D. A., M. J. Ackermann, J. R. Bischoff, D. H. Beach, and R. Peters.** 1991. p34cdc2-mediated phosphorylation at T124 inhibits nuclear import of SV-40 T antigen proteins. J. Cell Biol. **115**:1203–1212.
23. **Jetton, T. L., Y. Liang, C. C. Pettepher, E. C. Zimmerman, F. G. Cox, K. Horvath, F. M. Matschinsky, and M. A. Magnuson.** 1994. Analysis of upstream glucokinase promoter activity in transgenic mice and identification of glucokinase in rare neuroendocrine cells in the brain and gut. J. Biol. Chem. **269**:3641–3654.
24. **Jetton, T. L., and M. A. Magnuson.** 1992. Heterogeneous expression of glucokinase among pancreatic beta-cells. Proc. Natl. Acad. Sci. USA **89**:2619–2623.
25. **Kennelly, P. J., and E. G. Krebs.** 1991. Consensus sequences as substrate specificity determinants for protein kinases and protein phosphatases. J. Biol. Chem. **266**:15555–15558.
26. **Kidd, S.** 1992. Characterization of the Drosophila *cactus* locus and analysis of interactions between cactus and dorsal proteins. Cell **71**:623–635.
27. **Kinzler, K. W., J. M. Ruppert, S. H. Bigner, and B. Vogelstein.** 1988. The GLI gene is a member of the Kruppel family of zinc finger proteins. Nature (London) **332**:371–374.
28. **Kochoyan, M., T. F. Havel, D. T. Nguyen, C. E. Dahl, H. T. Keutmann, and M. A. Weiss.** 1991. Alternating zinc fingers in the human male associated protein ZFY; 2D NMR structure of an even finger and implications for "Jumper-Linker" DNA recognition. Biochemistry **30**:3371–3386.
29. **Kozak, M.** 1987. An analysis of 5′-noncoding sequences from 699 vertebrate messenger RNAs. Nucleic Acids Res. **15**:8125–8148.
30. **Kunkel, T. A.** 1985. Rapid and efficient site-specific mutagenesis without phenotype selection. Proc. Natl. Acad. Sci. USA **82**:488–492.
31. **Lehman, R., and C. Nusslein-Vollard.** 1987. *hunchback*, a gene required for segmentation of anterior and posterior regions of the *Drosophila* embryo. Dev. Biol. **119**:402–417.
32. **Lipkin, S. M., A. M. Naar, K. A. Kalla, R. A. Sack, and M. G. Rosenfeld.** 1993. Identification of a novel zinc finger protein binding a conserved element for Pit-1-dependent growth hormone gene expression. Genes Dev. **7**:1674–1687.
33. **Maniatis, T., E. F. Fritsch, and J. Sambrook.** 1989. Molecular cloning: a laboratory manual. Cold Spring Harbor Laboratory, Cold Spring Harbor, N.Y.

34. **Moll, T., G. Tebb, U. Surana, H. Robitsch, and K. Nasmyth.** 1991. The role of phosphorylation and the CDC28 protein kinase in cell cycle-regulated nuclear import of the S. cerevisiae transcription factor SWI5. Cell **66:**743–758.
35. **Morishita, K., D. S. Parker, M. L. Mucenski, N. A. Jenkins, N. G. Copeland, and J. N. Ihle.** 1988. Retroviral activation of a novel gene encoding a zinc finger protein in IL-3-dependent myeloid leukemia cell lines. Cell **54:**831–840.
36. **Nardelli, J., T. J. Gibson, C. Vesque, and P. Charnay.** 1991. Base sequence discrimination by zinc-finger DNA-binding domains. Nature (London) **349:**175–178.
37. **Norris, J. L., and J. L. Manley.** 1992. Selective nuclear transport of the *Drosophila* morphogen *dorsal* can be established by a signaling pathway involving the transmembrane protein *Toll* and protein kinase A. Genes Dev. **6:**1654–1667.
38. **Page, D. C., R. Mosher, E. M. Simpson, E. M. C. Fisher, G. Mardon, J. Pollack, B. McGillivray, A. de la Chapelle, and L. G. Brown.** 1987. The sex-determining region of the human Y chromosome encodes a finger protein. Cell **51:**1091–1104.
39. **Pavletich, N. P., and C. O. Pabo.** 1991. Zinc finger-DNA recognition: crystal structure of a Zif268-DNA complex at 2.1 A. Science **252:**809–817.
40. **Pavletich, N. P., and C. O. Pabo.** 1993. Crystal structure of a five-finger GLI-DNA complex: new perspectives on zinc fingers. Science **261:**1701–1707.
41. **Pevny, L., M. C. Simon, E. Robertson, W. H. Klein, S.-F. Tsai, V. D'Agati, S. H. Orkin, and F. Costantini.** 1991. Erythroid differentiation in chimaeric mice blocked by a targeted mutation in the gene for transcription factor GATA-1. Nature (London) **349:**257–260.
42. **Priess, A., U. B. Rosenberg, A. Kienlin, E. Seifert, and H. Jackle.** 1985. Molecular genetics of *Kruppel*, a gene required for segmentation of the *Drosophila* embryo. Nature (London) **313:**27–32.
43. **Prives, C.** 1990. The replication functions of SV40 T antigen are regulated by phosphorylation. Cell **61:**735–738.
44. **Read, D., and J. L. Manley.** 1992. Alternatively spliced transcripts of the *Drosophila tramtrack* gene encode zinc finger proteins with distinct DNA binding specificities. EMBO J. **11:**1035–1044.
45. **Reuter, G., M. Giarre, J. Farah, J. Gausz, A. Spierer, and P. Spierer.** 1990. Dependence of position-effect variegation in Drosophila on dose of a gene encoding an unusual zinc-finger protein. Nature (London) **244:**219–223.
46. **Rihs, H.-P., D. A. Jans, H. Fan, and R. Peters.** 1991. The rate of nuclear cytoplasmic protein transport is determined by the casein kinase II site flanking the nuclear localization of the SV40 T-antigen. EMBO J. **10:**633–639.
47. **Rosenberg, U. B., C. Schroder, A. Priess, A. Kienlin, S. Cote, J. Riede, and H. Jackle.** 1986. Structural homology of the product of the Drosophila *Kruppel* gene with Xenopus transcription factor IIIA. Nature (London) **319:**336–339.
48. **Ruiz i Altaba, A., H. Perry-O'Keefe, and D. A. Melton.** 1987. Xfin: an embryonic gene encoding a multifingered protein in Xenopus. EMBO J. **6:**3065–3070.
49. **Ruppert, J. M., B. Vogelstein, K. Arheden, and K. Kinzler.** 1990. *GLI3* encodes a 190-kilodalton protein with multiple regions of GLI similarity. Mol. Cell. Biol. **10:**5408–5415.
50. **Schuh, R., W. Aicher, U. Gaul, S. Coté, A. Priess, D. Maier, E. Seifert, U. Nauber, C. Schröeder, and R. Kemler.** 1986. A conserved family of nuclear proteins containing the structural elements of the finger protein encoded by *kruppel*, a *drosophila* segmentation gene. Cell **47:**1025–1032.
51. **Settleman, J., V. Narasimhan, L. C. Foster, and R. A. Weinberg.** 1992. Molecular cloning of cDNAs encoding the GAP-associated protein p190: implications for a signaling pathway from *Ras* to the nucleus. Cell **69:**539–549.
52. **Shaw, G., and R. Kamen.** 1986. A conserved AU sequence from the 3′-untranslated region of GM-CSF mRNA mediates selective mRNA degradation. Cell **46:**659–667.
53. **Shelton, K. D., A. Franklin, A. Khoor, J. Beechem, and M. A. Magnuson.** 1992. Multiple elements in the upstream glucokinase promoter are necessary for transcription in insulinoma cells. Mol. Cell. Biol. **12:**4578–4589.
54. **Singh, H., J. H. LeBowitz, A. S. Baldwin, and P. A. Sharp.** 1988. Molecular cloning of an enhancer binding protein: isolation by screening of an expression library with a recognition site probe. Cell **52:**415–423.
55. **Smith, D. B., and K. S. Johnson.** 1988. Single step purification of polypeptides expressed in *Escherichia coli* as fusions with glutathione S-transferase. Gene **67:**31–40.
56. **Steward, R.** 1989. Relocalization of the *dorsal* protein from the cytoplasm to the nucleus correlates with its function. Cell **59:**1179–1188.
57. **Steward, R., S. B. Zusman, L. H. Huang, and P. Schedl.** 1988. The *dorsal* protein is distributed in a gradient in early Drosophila embryos. Cell **55:**487–495.
58. **Stillman, D. J., A. T. Bankier, A. Seddon, E. G. Groenhout, and K. A. Nasmyth.** 1988. Characterization of a transcription factor involved in mother cell specific transcription of the yeast *HO* gene. EMBO J. **7:**485–494.
59. **Sukhatme, V. P., X. Cao, L. C. Chang, C.-H. Tsai-Morris, D. Stamenkovich, P. C. Ferreira, D. R. Cohen, S. A. Edwards, T. B. Shows, T. Curran, M. M. Le Beau, and E. D. Adamson.** 1988. A zinc finger-encoding gene coregulated with c-fos during growth and differentiation, and after cellular depolarization. Cell **53:**37–43.
60. **Tautz, D., R. Lehmann, H. Schnurch, R. Schuh, E. Seifert, A. Kienlin, K. Jones, and H. Jackle.** 1987. Finger protein of novel structure encoded by *hunchback*, a second member of the gap class of Drosophila segmentation genes. Nature (London) **327:**383–389.
61. **Tsai, S.-F., D. I. Martin, L. I. Zon, A. D. d'Andrea, G. G. Wong, and S. H. Orkin.** 1989. Cloning of cDNA for the major DNA-binding protein of the erythroid lineage through expression in mammalian cells. Nature (London) **339:**446–451.
62. **Vinson, C. R., K. L. LaMarco, P. F. Johnson, W. H. Landschultz, and S. L. McNight.** 1988. In situ detection of sequence-specific DNA-binding specified by a recombinant bacteriophage. Genes Dev. **2:**801–806.
63. **Vortkamp, A., M. Gessler, and K.-H. Grzeschik.** 1991. GLI3 zinc-finger gene interrupted by translocations in Grieg syndrome families. Nature (London) **352:**539–540.
64. **Vriz, S., J.-M. Lemaitre, M. Leibovici, N. Thierry, and M. Mechali.** 1992. Comparative analysis of the intracellular localization of c-Myc, c-Fos, and replicative proteins during cell cycle progression. Mol. Cell. Biol. **12:**3548–3555.
65. **Wingender, E.** 1990. Transcription regulating proteins and their recognition sequences. Crit. Rev. Eukaryotic Gene Expression **1:**11–48.